Squared form factors of vibronic excitations in 12–13.3 eV of nitrogen studied by high-resolution inelastic x-ray scattering

Yi-Geng Peng,[1] Xu Kang,[1] Ke Yang,[2,*] Xiao-Li Zhao,[1] Ya-Wei Liu,[1] Xiao-Xun Mei,[1] Wei-Qing Xu,[1] Nozomu Hiraoka,[3] Ku-Ding Tsuei,[3] and Lin-Fan Zhu[1,†]

[1]*Hefei National Laboratory for Physical Sciences at Microscale, Department of Modern Physics, University of Science and Technology of China, Hefei, Anhui 230026, People's Republic of China*
[2]*Shanghai Institute of Applied Physics, Chinese Academy of Sciences, Shanghai 201204, People's Republic of China*
[3]*National Synchrotron Radiation Research Center, Hinchu 300376, Taiwan, Republic of China*

Vibronically resolved squared form factors of $a'' \, ^1\Sigma_g{}^+$, $b \, ^1\Pi_u$, $b' \, ^1\Sigma_u{}^+$, $c_3 \, ^1\Pi_u$, $c_4' \, ^1\Sigma_u{}^+$, and $o_3 \, ^1\Pi_u$ of molecular nitrogen are determined by inelastic x-ray scattering with a high resolution of 70 meV. Through a comparison with the previous results measured by electron energy loss spectroscopy, it is found that the first Born approximation is satisfied at an incident electron energy of 300 eV in the small momentum transfer region for a dipole-allowed transition of $b \, ^1\Pi_u$, but the first Born approximation is not reached at an impact energy of 500 eV for the dipole-forbidden transition of $a'' \, ^1\Sigma_g{}^+$. It is also observed from the present experimental results that the momentum transfer dependence behavior of the excitations to $b \, ^1\Pi_u(\nu' = 3,4)$ is different from that of the excitations to $b \, ^1\Pi_u(\nu' = 1,2)$, which can be attributed to the perturbation of $c_3 \, ^1\Pi_u$ to $b \, ^1\Pi_u$. The present results provide experimental benchmark data of inelastic squared form factors of molecular nitrogen.

PACS number(s): 33.20.Rm, 33.70.Ca, 34.50.Gb

I. INTRODUCTION

As a main component of the earth's atmosphere, nitrogen has attracted the interest of physicists and chemists and its excitation dynamic parameters have been measured and calculated extensively. Traditionally, the excitation dynamic parameters, such as the photoabsorption cross sections, differential cross sections (DCSs), and the generalized oscillator strengths (GOSs), for the valence-shell excitations of nitrogen were measured by the photoabsorption method and electron energy loss spectroscopy (EELS). The photoabsorption cross section reveals the character of a wave function at large scales because it is measured at very small momentum transfer, whereas the wave function at all length scales can be explored by the electron-impact method since the momentum transfers that rely on the scattering angles can be varied in the collision process. Especially for the high-energy electron impact, it is generally thought that the first Born approximation (FBA) is satisfied and the experimental DCS can be converted into a GOS, which is proportional to the squared transition matrix element. So for a long time the high-energy EELS has been used as a tool to explore the structure of an atom or a molecule, i.e., the information of wave functions of its ground and excited states. However, recent inelastic x-ray scattering (IXS) studies [1–3] show that the high-order Born amplitude makes a considerable contribution to the experimental DCSs in the electron-impact method, even at a high impact energy of several keV. Since the FBA is nearly always satisfied in IXS, the inelastic squared form factors (ISFFs) measured by IXS provide an experimental benchmark to test theoretical methods [4–8] stringently. This is the main purpose of the present work.

The excitation energy range of nitrogen interested in this work is 12–13.3 eV, where the vibronic excitations to $a'' \, ^1\Sigma_g{}^+(\nu' = 0$–$1)$, $b \, ^1\Pi_u(\nu' = 0$–$9)$, $b' \, ^1\Sigma_u{}^+(\nu' = 0$–$4)$, $c_3 \, ^1\Pi_u(\nu' = 0$–$1)$, $c_4' \, ^1\Sigma_u{}^+(\nu' = 0$–$1)$, and $o_3 \, ^1\Pi_u(\nu' = 0$–$1)$ are located. The differential cross sections of the aforementioned transitions have been studied by EELS experiments, including the ones carried out at low impact energies (<100 eV) [9–20], moderate impact energies (100–600 eV) [21–24], and high impact energies (0.6–25 keV) [3,25]. In the EELS studies of Refs. [21,22,25] and the IXS one of Ref. [3], the low-experimental-energy resolutions (more than 1 eV) obstruct them to resolve the vibronic structures. The good energy resolutions in Refs. [23,24,26] are high enough to explore the vibronic structures of $a'' \, ^1\Sigma_g{}^+$ and $b \, ^1\Pi_u$, but the largest momentum transfer achieved by them is relatively small and the incident electron energies of 300–500 eV in Refs. [23,24,26] may not be high enough to approach the FBA. Thus high-energy EELS or IXS investigations with high-energy resolution for the aforementioned vibronic valence-shell excitations of nitrogen are lacking.

Compared with the large body of existing experimental works, there are few theoretical calculations [12,27–29]. Among them, the early theoretical calculation of Chung and Lin [27], Rozsnyai [28], and Domenicucci and Miller [29] may not be accurate enough because of the limited calculation ability at that time, since the strong configuration interactions among different electronic states that result in the avoid crossing of potential curves were not taken into account. It is well known that for an electronic state that is perturbed by a nearby state, e.g., $B \, ^1\Sigma^+$ of CO and $E \, ^3\Sigma_u{}^-$ of O_2, the apparent GOSs of its different vibronic states will show apparently different momentum transfer dependence behaviors [30–33]. Recently, a similar momentum transfer dependence behavior of $b \, ^1\Pi_u$ of N_2 was investigated by Heays *et al.* [12], who calculated the GOS ratios of all vibronic states of $b \, ^1\Pi_u$ to $b \, ^1\Pi_u(\nu' = 2)$ using the coupled-channel model. In their

calculations the strong interaction between the Rydberg state of $c_3\,^1\Pi_u$ and the valence state of $b\,^1\Pi_u$ was considered carefully. However, they only calculated the GOS ratios in the lower momentum transfer region.

The ISFF is defined as

$$\zeta(\mathbf{q},\omega_n) = \left| \langle \Psi_n | \sum_{j=1}^{N} \exp(i\mathbf{q}\cdot\mathbf{r}_j) | \Psi_0 \rangle \right|^2. \tag{1}$$

Here $\mathbf{q}$ is the momentum transfer and Ψ_0 and Ψ_n are the wave functions of the initial and final states, respectively. The sum is over all electrons and $\mathbf{r}_j$ is the position vector of the jth electron. The ISFF can be determined from the differential cross section measured by the IXS and the high-energy EELS under the condition that the FBA is valid:

$$\begin{aligned}\zeta(\mathbf{q},\omega_n) &= \frac{1}{r_0^2}\frac{\omega_i}{\omega_f}\frac{1}{|\boldsymbol{\epsilon}_i\cdot\boldsymbol{\epsilon}_f^*|^2}\left(\frac{d\sigma}{d\Omega}\right)_\gamma \\ &= \frac{1}{4}\frac{k_i}{k_f}q^4\left(\frac{d\sigma}{d\Omega}\right)_e \\ &= \frac{q^2}{2\omega_n}f(\mathbf{q},\omega_n). \end{aligned} \tag{2}$$

The factor $|\boldsymbol{\epsilon}_i\cdot\boldsymbol{\epsilon}_f^*|^2$ comes from the polarized direction of incident and scattered photons and it equals $\cos^2 2\theta$ (2θ is the scattering angle) for completely linear polarized photons with the polarized direction in the horizontal scattering plane. Here r_0 is the classical electron radius; ω_i, ω_f, and $\omega_n = \omega_i - \omega_f$ stand for the energies of the incident photon, scattered photon, and energy loss, respectively; $(\frac{d\sigma}{d\Omega})_\gamma$ and $(\frac{d\sigma}{d\Omega})_e$ stand for the DCSs measured by the IXS and the high-energy EELS, respectively; $f(\mathbf{q},\omega_n)$ is the generalized oscillator strength, which is a commonly used quantity in the high-energy EELS; and k_i and k_f are the momenta of the incident and the scattered electrons respectively.

In the present paper the inelastic squared form factors for the vibronic excitations of $a''\,^1\Sigma_g^+$, $b\,^1\Pi_u$, $b'\,^1\Sigma_u^+$, $c_3\,^1\Pi_u$, $c_4'\,^1\Sigma_u^+$, and $o_3\,^1\Pi_u$ of N_2 are measured by high-resolution (70-meV) IXS. The squared momentum transfer q^2 is from near 0 to 5 a.u.

II. EXPERIMENTAL METHOD

The present experiment was carried out at Taiwan Beamline BL12XU of SPring-8. The experimental setup and method used in this work were described in our previous works [1,2,34,35] in detail. Briefly, the energy for the scattered photon was fixed at 9888.8 eV, while the incident photon energy varied, from which the energy loss is determined. The energy resolution of this work is about 70 meV and a typical IXS spectrum of nitrogen is shown in Fig. 1 along with the vibronic states assigned. It can be seen clearly from Fig. 1 that the measured spectrum is vibronically resolved. In order to determine the intensity of individual vibronic excitation, a least-squares fitting was used to fit the experimental spectra. In the fitting procedure, the energy positions of the vibronic excitations were fixed to the ones summarized by Khakoo *et al.* [10] and the peak profile was described by a Gaussian function. The fitted results are satisfactory and are shown in
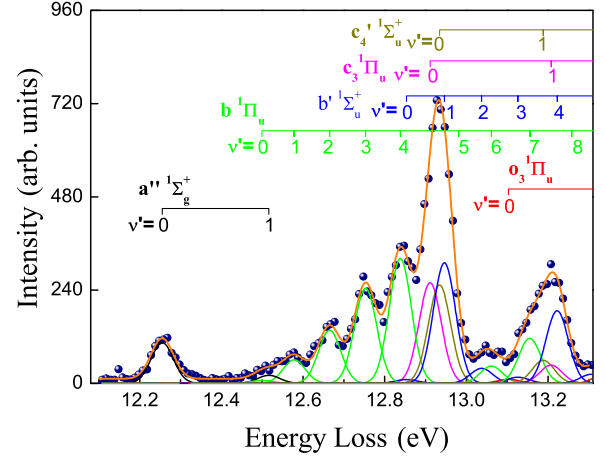

FIG. 1. (Color online) Typical IXS spectrum of the valence-shell excitations of molecular nitrogen at 9° ($q^2 \approx 0.17$ a.u.). Solid lines are the fitted curves.

Fig. 1. Because the energy interval between $a''\,^1\Sigma_g^+(v'=1)$ and $b\,^1\Pi_u(v'=0)$ is less than the present energy resolution, the sum of their intensities was used to determine the total ISFF of these two states. Similarly, the intensities of $b\,^1\Pi_u(v'=4) + b'\,^1\Sigma_u^+(v'=0)$, $c_3\,^1\Pi_u(v'=0) + b\,^1\Pi_u(v'=5) + c_4'\,^1\Sigma_u^+ (v'=0) + b'\,^1\Sigma_u^+(v'=1)$, $b\,^1\Pi_u(v'=6) + b'\,^1\Sigma_u^+(v'=2)$, $o_3\,^1\Pi_u(v'=0) + b\,^1\Pi_u(v'=7) + b'\,^1\Sigma_u^+(v'=3)$, and $c_3\,^1\Pi_u(v'=1) + b\,^1\Pi_u(v'=8) + c_4'\,^1\Sigma_u^+(v'=1) + b'\,^1\Sigma_u^+ (v'=4)$ were obtained.

Herein $\zeta(\mathbf{q},\omega_n)$ for the $1s^2 \rightarrow 1s2p$ transition of helium, which has been measured and calculated with high accuracy and proven to be reliable [34,36–38], was measured in small scattering angles and used to normalize the results of nitrogen. In the normalization procedure, the different target densities of helium (8.00 atm) and nitrogen (9.00 atm) as well as their actual transmission rates were measured and used to absolutize the experimental data obtained for the same experimental conditions. The ISFFs for the valence-shell vibronic excitations of nitrogen were determined and are listed in Table I. The experimental errors of the ISFFs, which are also listed in Table I and shown in corresponding figures, are attributed to the statistics of counts, the fitting procedure, and the normalizing procedure.

III. RESULTS AND DISCUSSION

The present ISFFs are shown in Figs. 2–5 along with the available previous experimental results. The present results are fitted by

$$\zeta(\mathbf{q},\omega_n) = \frac{q^2}{2\omega_n}\frac{x^M}{(1+x)^{(l+l'+m+5)}}\sum_{m=0}^{\infty}\frac{f_m x^m}{(1+x)^m}. \tag{3}$$

Formula (3) is obtained by modifying a formula that is used to fit the GOS and proposed by Lassettre and Klump [39,40] based on Eq. (2). Here $x = q^2/\alpha^2$, with α a quantity relevant to the excitation energy and the ionization energy of the target, here regarded as a fitting parameter. In addition, l and l' are the orbital angular momenta of the initial and final

TABLE I. The present ISFFs determined by the IXS. The listed data are amplified a factor of 10^3. Data in the parentheses are the corresponding experimental uncertainties. For clarity, the vibronic states are represented by their term names and vibrational numbers, such as $a'' \, {}^1\Sigma_g^+(v'=0)$ being written as $a''(0)$.

q^2 (a.u.)	$a''(0)$	$a''(1)+b(0)$	$b(1)$	$b(2)$	$b(3)$	$b(4)+b'(0)$
0.05	0.37(0.08)	0.21(0.08)	0.59(0.08)	1.33(0.10)	2.50(0.13)	3.91(0.19)
0.11	1.16(0.12)	0.43(0.11)	1.03(0.12)	2.54(0.14)	4.42(0.18)	6.54(0.25)
0.17	2.70(0.19)	0.73(0.17)	1.57(0.18)	3.54(0.19)	6.33(0.24)	8.58(0.31)
0.26	4.77(0.33)	0.97(0.29)	1.94(0.31)	4.49(0.31)	7.00(0.33)	10.4(0.49)
0.36	5.81(0.30)	1.22(0.26)	2.18(0.27)	4.97(0.27)	7.85(0.30)	10.9(0.45)
0.48	7.79(0.31)	[a]	2.49(0.30)	5.04(0.30)	8.47(0.34)	10.7(0.45)
0.65	8.99(0.34)	1.58(0.28)	2.55(0.29)	5.61(0.29)	9.52(0.32)	10.7(0.40)
0.85	7.99(0.35)	1.65(0.28)	2.36(0.29)	5.45(0.29)	7.42(0.31)	8.37(0.42)
1.22	6.45(0.38)	1.70(0.33)	2.26(0.33)	4.82(0.34)	6.51(0.35)	6.49(0.43)
1.65	5.37(0.47)	1.39(0.42)	1.98(0.43)	4.03(0.41)	5.74(0.43)	4.80(0.57)
2.63	5.26(0.47)	0.93(0.58)	1.41(0.57)	3.88(0.57)	5.42(0.59)	3.84(0.68)
3.55	4.32(0.65)	0.65(0.55)	2.18(0.60)	2.66(0.54)	3.71(0.58)	2.65(0.74)
4.77	3.47(0.58)	0.44(0.50)	1.54(0.53)	2.83(0.50)	4.01(0.55)	2.35(0.63)
q^2 (a.u.)	$c_3(0)+b(5)+c_4'(0)+b'(1)$	$b(6)+b'(2)$	$o_3(0)+b(7)+b'(3)$	$c_3(1)+b(8)+c_4'(1)+b'(4)$		
0.05	10.9(0.47)	0.56(0.13)	1.14(0.60)	3.31(0.43)		
0.11	18.0(0.59)	1.32(0.18)	2.61(0.79)	5.47(0.61)		
0.17	21.3(0.61)	2.15(0.29)	3.7(1.2)	7.59(0.88)		
0.26	21.2(0.66)	2.62(0.54)	4.4(2.3)	9.6(1.6)		
0.36	18.8(0.56)	3.58(0.52)	5.2(2.3)	10.7(1.6)		
0.48	15.3(0.55)	4.71(1.03)	6.2(2.2)	11.8(2.3)		
0.65	10.6(0.45)	6.26(0.5)	9.4(1.4)	10.7(1.0)		
0.85	6.17(0.46)	7.26(0.6)	10.0(2.0)	9.8(1.5)		
1.22	4.59(0.51)	10.7(0.8)	9.6(1.6)	9.5(1.1)		
1.65	4.86(0.66)	11.5(1.4)	10.7(2.9)	7.8(2.0)		
2.63	6.48(0.92)	11.5(2.3)	12.0(3.0)	8.2(1.8)		
3.55	7.19(0.94)	12.5(2.4)	10.8(6.4)	6.8(5.9)		
4.77	7.00(0.83)	9.6(1.7)	10.1(4.4)	8.4(3.0)		

[a]This point is absent because the electron beam was aborted.

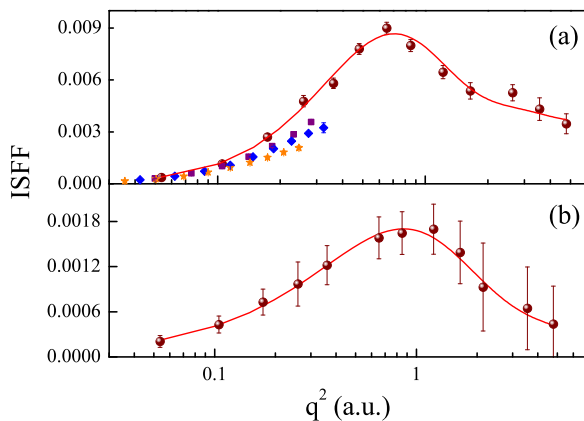states, respectively, and M is a quantity that is relevant to the excitation multipolarity [40,41].

FIG. 2. (Color online) The ISFFs for excitations to (a) $a'' \, {}^1\Sigma_g^+(v'=0)$ and (b) $a'' \, {}^1\Sigma_g^+(v'=1)+b \, {}^1\Pi_u(v'=0)$. Dots are the present IXS results; stars, diamonds, and squares are the EELS results measured at incident electron energies of 300, 400, and 500 eV by Skerbele and Lassettre [23]; and solid lines are the fitted results.

Figure 2(a) shows the present ISFF for the excitation to $a'' \, {}^1\Sigma_g^+(v'=0)$ along with the EELS ones of Skerbele and Lassettre [23] and the fitted curve. It can be seen clearly that the results of Ref. [23] are lower than the present ones and the EELS results with the increasing impact energies are getting larger. This phenomenon means that the FBA is not satisfied at an impact energy of 500 eV for the excitation to $a'' \, {}^1\Sigma_g^+(v'=0)$. Figure 2(b) shows the total ISFF of $a'' \, {}^1\Sigma_g^+(v'=1)+b \, {}^1\Pi_u(v'=0)$. For these two excitations moderate- or high-energy EELS results are lacking.

Figure 3 shows the present ISFFs for the excitations to $b \, {}^1\Pi_u(v'=1-3)$ and $b \, {}^1\Pi_u(v'=4)+b' \, {}^1\Sigma_u^+(v'=0)$ as well as the EELS results measured at 300 eV by Xu *et al.* [24]. In Ref. [24], the reported GOS of $b \, {}^1\Pi_u(v'=4)$ should include the contribution of $b' \, {}^1\Sigma_u^+(v'=0)$ because the energy interval is less than their energy resolution. It can be seen from Fig. 3 that the present ISFFs are in good agreement with the EELS ones at 300 eV in the small-q^2 region, i.e., $q^2 < 0.5$ a.u. for $b \, {}^1\Pi_u(v'=1,2)$, $q^2 < 0.4$ a.u. for $b \, {}^1\Pi_u(v'=3)$, and $q^2 < 0.22$ a.u. for $b \, {}^1\Pi_u(v'=4)+b' \, {}^1\Sigma_u^+(v'=0)$, considering the mutual uncertainties, which means that the FBA is reached in these q^2 region at an incident electron energy of 300 eV for these excitations. However, the EELS results in the large-q^2 range begin to oscillate evidently. This may be due to the
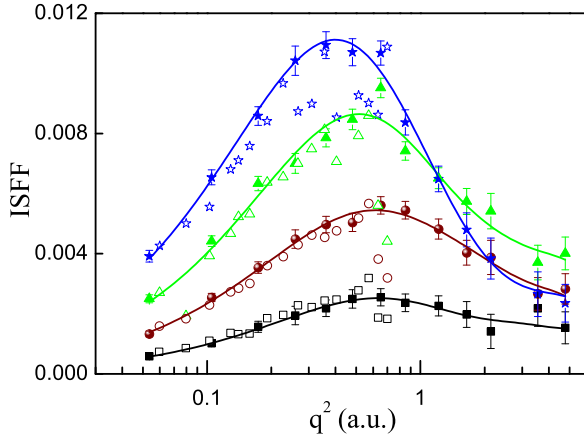
FIG. 3. (Color online) The ISFFs for the vibronic excitations to $b\,^1\Pi_u$. Closed symbols are the present IXS results: squares, $v' = 1$; circles, $v' = 2$; triangles, $v' = 3$; and stars, $v' = 4$ [including the contribution of $b'\,^1\Sigma_u^+(v' = 0)$]. The corresponding open symbols are the EELS results measured at an incident electron energy of 300 eV [24]. Solid lines are the fitted curves.

invalidity of the FBA in this q^2 region or the very low DCSs of the electron-impact method since it is proportional to q^{-4}, while IXS is free from this disadvantage, as pointed out by Refs. [1,2,34,35].

It is well known that the intensities of different vibronic states in one electronic state are proportional to the Franck-Condon factors and generally the intensity ratio of any two vibronic states belonging to the same electronic state is independent of the momentum transfer. Figure 4 shows the present ISFF ratios of $b\,^1\Pi_u(v' = 1,3)$ and $b\,^1\Pi_u(v' = 4) + b'\,^1\Sigma_u^+(v' = 0)$ to $b\,^1\Pi_u(v' = 2)$ along with the calculated ones by Heays *et al.* [12]. Although the resolution of the present work is not high enough to resolve $b\,^1\Pi_u(v' = 4)$ and $b'\,^1\Sigma_u^+(v' = 0)$, the contribution of $b'\,^1\Sigma_u^+(v' = 0)$ to $b\,^1\Pi_u(v' = 4)$ in $q^2 < 1.2$ a.u. can be ignored since the intensity of $b'\,^1\Sigma_u^+(v' = 0)$ is much smaller than that of $b\,^1\Pi_u(v' = 4)$
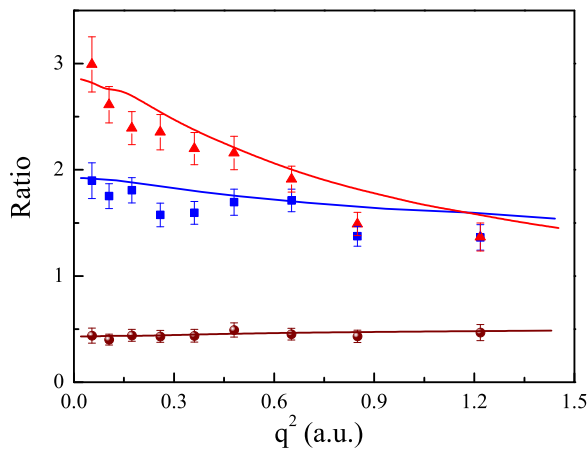

FIG. 4. (Color online) Present ISFF ratios of $b\,^1\Pi_u(v' = 1, 3,$ and 4) to $b\,^1\Pi_u(v' = 2)$. Dots, squares, and triangles represent the ratios of $b\,^1\Pi_u(v' = 1, 3,$ and 4). Solid lines are the calculated results of Heays *et al.* [12].
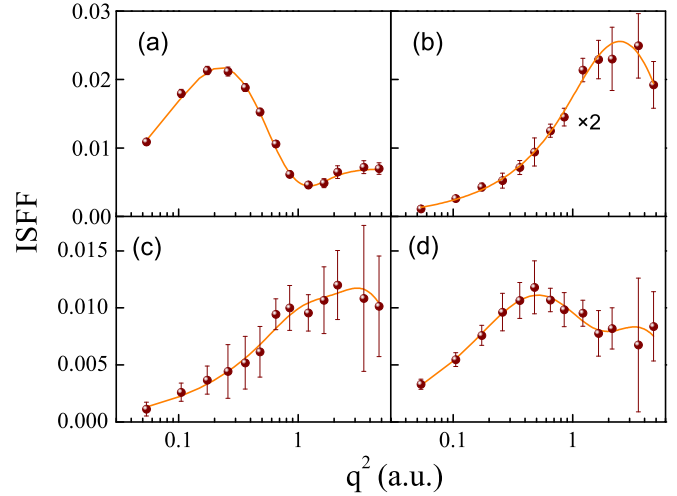

FIG. 5. (Color online) Present ISFFs for excitations to (a) $c_3\,^1\Pi_u(v' = 0) + b\,^1\Pi_u(v' = 5) + c_4'\,^1\Sigma_u^+(v' = 0) + b'\,^1\Sigma_u^+(v' = 1)$, (b) $b\,^1\Pi_u(v' = 6) + b'\,^1\Sigma_u^+(v' = 2)$, (c) $o_3\,^1\Pi_u(v' = 0) + b\,^1\Pi_u(v' = 7) + b'\,^1\Sigma_u^+(v' = 3)$, and (d) $c_3\,^1\Pi_u(v' = 1) + b\,^1\Pi_u(v' = 8) + c_4'\,^1\Sigma_u^+(v' = 1) + b'\,^1\Sigma_u^+(v' = 4)$. Dots are the present IXS results and solid lines are the fitted curves.

[10,42]. It is clear from Fig. 4 that the experimental and theoretical ratios of $b\,^1\Pi_u(v' = 1)$ to $b\,^1\Pi_u(v' = 2)$ are in good agreement and the ratios are nearly a horizontal line, which means that these two vibronic states follow the Franck-Condon approximation. However, the present ISFF ratios of $b\,^1\Pi_u(v' = 3,4)$ to $b\,^1\Pi_u(v' = 2)$ vary with the momentum transfer, which means that for $b\,^1\Pi_u(v' = 3,4)$ the Franck-Condon approximation is broken and the theoretical calculations show a similar momentum transfer dependence behavior. The reason for this phenomenon should be due to the interactions between $b\,^1\Pi_u$ and $c_3\,^1\Pi_u$, which result in the avoid crossing of these two potential curves. Since $v' = 1$ and 2 of $b\,^1\Pi_u$ are far from the avoid-crossing point, for these two vibronic states their ISFF ratios observe the Franck-Condon approximation. However, since $v' = 3$ and 4 of $b\,^1\Pi_u$ are close to the avoid-crossing point, the corresponding ISFF ratios of $v' = 3$ and 4 to $v' = 2$ are dependent on the momentum transfer. Similar phenomena were also observed and studied for the valence-shell excitations of oxygen and carbon monoxide [30–33]. It can also be noticed from Fig. 4 that there is a noticeable difference between the experimental ISFF ratios of $v' = 3$ and 4 to $v' = 2$ and the calculated ones by Ref. [12]. The ISFF ratios of $v' = 5,6,7,\ldots$ to $v' = 2$ calculated by Ref. [12] are also dependent on the q^2; however, limited by the present energy resolution, we cannot obtain reliable ISFF ratios for $v' = 5,6,7,\ldots$ to $v' = 2$. So further high-energy resolution experimental measurements and highly accurate theoretical calculations are strongly recommended.

Figure 5 shows the present ISFFs for vibronic excitations that cannot be resolved at the present energy resolution; there are no other theoretical calculation and experimental result to compare them with. To obtain the quantitative ISFF for individual vibronic excitation in Fig. 5, a much higher energy resolution is needed. We hope that this kind of experiment can be done in the near future with the development of the third-generation synchrotron radiation.

IV. CONCLUSION

The high-resolution IXS method was used to investigate the ISFFs of vibronic excitations in 12–13.3 eV of nitrogen. Since the FBA is satisfied in the IXS, the present ISFFs for valence-shell excitations of N_2 can be used as the experimental benchmark data to test the validity of the FBA in the EELS method. In particular, by comparing the present IXS results with the EELS ones of Skerbele and Lassettre [23] and Xu *et al.* [24], it was found that for $a'' \, ^1\Sigma_g^+$ the FBA has not been reached at an incident electron energy of 500 eV, while for $b \, ^1\Pi_u (v' = 1 - 4)$ the FBA is satisfied in the small-q^2 region at $E_0 = 300$ eV. The non-Franck-Condon phenomena due to the interaction between $b \, ^1\Pi_u$ and $c_3 \, ^1\Pi_u$ were observed from the measured ISFF ratios of $b \, ^1\Pi_u (v' = 3,4)$ to $b \, ^1\Pi_u (v' = 2)$. High-energy-resolution experiments and accurate theoretical calculation are strongly recommended to explore the interac-tions between different electronic states as well as the dynamic behaviors of higher excited states.

[1] X. Kang, K. Yang, Y. W. Liu, W. Q. Xu, N. Hiraoka, K. D. Tsuei, P. F. Zhang, and L. F. Zhu, Phys. Rev. A **86**, 022509 (2012).

[2] L. F. Zhu, W. Q. Xu, K. Yang, Z. Jiang, X. Kang, B. P. Xie, D. L. Feng, N. Hiraoka, and K. D. Tsuei, Phys. Rev. A **85**, 030501(R) (2012).

[3] J. A. Bradley, G. T. Seidler, G. Cooper, M. Vos, A. P. Hitchcock, A. P. Sorini, C. Schlimmer, and K. P. Nagle, Phys. Rev. Lett. **105**, 053202 (2010).

[4] A. Sakko, A. Rubio, M. Hakala, and K. Hamalainen, J. Chem. Phys. **133**, 174111 (2010).

[5] A. Sakko, S. Galambosi, J. Inkinen, T. Pylkkanen, M. Hakala, S. Huotari, and K. Hamalainen, Phys. Chem. Chem. Phys. **13**, 11678 (2011).

[6] A. N. Hopersky, A. M. Nadolinsky, K. K. Ikoeva, and O. A. Khoroshavina, J. Phys. B **44**, 145202 (2011).

[7] A. N. Hopersky, A. M. Nadolinsky, S. A. Novikov, and V. A. Yavna, J. Phys. B **46**, 155202 (2013).

[8] A. N. Hopersky, A. M. Nadolinsky, K. K. Ikoeva, and O. A. Khoroshavina, J. Exp. Theor. Phys. **113**, 731 (2011).

[9] M. A. Khakoo, P. V. Johnson, I. Ozkay, P. Yan, S. Trajmar, and I. Kanik, Phys. Rev. A **71**, 062703 (2005).

[10] M. A. Khakoo, C. P. Malone, P. V. Johnson, B. R. Lewis, R. Laher, S. Wang, V. Swaminathan, D. Nuyujukian, and I. Kanik, Phys. Rev. A **77**, 012704 (2008).

[11] C. P. Malone, P. V. Johnson, I. Kanik, B. Ajdari, and M. A. Khakoo, Phys. Rev. A **79**, 032704 (2009).

[12] A. N. Heays, B. R. Lewis, S. T. Gibson, C. P. Malone, P. V. Johnson, I. Kanik, and M. A. Khakoo, Phys. Rev. A **85**, 012705 (2012).

[13] G. Joyez, R. I. Hall, J. Reinhardt, and J. Mazeau, J. Electron Spectrosc. Relat. Phenom. **2**, 183 (1973).

[14] M. Furlan, M. J. Hubin-Franskin, J. Delwichet, and J. E. Collin, J. Phys. B **23**, 3023 (1990).

[15] M. Zubek and G. C. King, J. Phys. B **27**, 2613 (1994).

[16] A. Hirabayashi and A. Ichimura, J. Phys. Soc. Jpn. **60**, 862 (1991).

[17] D. G. Wilden, P. J. Hicks, and J. Comer, J. Phys. B **12**, 1579 (1979).

[18] A. J. Williams and J. P. Doering, J. Chem. Phys. **51**, 2859 (1969).

[19] E. N. Lassettre, A. Skerbele, M. A. Dillon, and K. J. Ross, J. Chem. Phys. **48**, 5066 (1968).

[20] D. C. Cartwright, A. Chutjian, S. Trajmar, and W. Williams, Phys. Rev. A **16**, 1013 (1977).

[21] S. M. Silverman and E. N. Lassettre, J. Chem. Phys. **42**, 3420 (1965).

[22] E. N. Lassettre and M. E. Krasnow, J. Chem. Phys. **40**, 1248 (1964).

[23] A. Skerbele and E. N. Lassettre, J. Chem. Phys. **53**, 3806 (1970).

[24] K. Z. Xu, Z. P. Zhong, S. L. Wu, R. F. Feng, S. Ohtani, T. Takayanagi, and A. Kimota, Sci. China Ser. A **38**, 368 (1995).

[25] T. C. Wong, J. S. Lee, H. F. Wellenstein, and R. A. Bonham, J. Chem. Phys. **63**, 1538 (1975).

[26] E. N. Lassettre, A. Skerbele, and V. D. Meyer, J. Chen. Phys. **45**, 3214 (1966).

[27] S. Chung and C. C. Lin, Phys. Rev. A **6**, 988 (1972).

[28] B. F. Rozsnyai, J. Chem. Phys. **47**, 4102 (1967).

[29] A. G. Domenicucci and K. J. Miller, J. Chem. Phys. **66**, 3927 (1977).

[30] M. Kimura, M. A. Dillon, R. J. Buenker, G. Hirsch, Y. Li, and L. Chantranupong, Z. Phys. D **38**, 165 (1996).

[31] M. Dillon, M. Kimura, R. J. Buenker, G. Hirsch, Y. Li, and L. Chantranupong, J. Chem. Phys. **102**, 1561 (1995).

[32] B. R. Lewis, J. P. England, S. T. Gibson, M. J. Brunger, and M. Allan, Phys. Rev. A **63**, 022707 (2001).

[33] Y. Li, M. Honigmann, K. Bhanuprakash, G. Hirsch, R. J. Buenker, M. A. Dillon, and M. Kimura, J. Chem. Phys. **96**, 8314 (1992).

[34] B. P. Xie, L. F. Zhu, K. Yang, B. Zhou, N. Hiraoka, Y. Q. Cai, Y. Yao, C. Q. Wu, E. L. Wang, and D. L. Feng, Phys. Rev. A **82**, 032501 (2010).

[35] L. F. Zhu, L. S. Wang, B. P. Xie, K. Yang, N. Hiraoka, Y. Q. Cai, and D. L. Feng, J. Phys. B **44**, 025203 (2011).

[36] X. Y. Han and J. M. Li, Phys. Rev. A **74**, 062711 (2006).

[37] X. J. Liu, L. F. Zhu, Z. S. Yuan, W. B. Li, H. D. Cheng, J. M. Sun, and K. Z. Xu, J. Electron Spectrosc. Relat. Phenom. **135**, 15 (2004).

[38] N. M. Cann and A. J. Thakkar, J. Electron Spectrosc. Relat. Phenom. **123**, 143 (2002).

[39] E. N. Lassettre, J. Chem. Phys. **43**, 4479 (1965).

[40] K. N. Klump and E. N. Lassettre, J. Chem. Phys. **68**, 886 (1978).

[41] A. R. P. Rau and U. Fano, Phys. Rev. **162**, 68 (1967).

[42] D. Stahel, M. Leoni, and K. Dressler, J. Chem. Phys. **79**, 2541 (1983).